The Torun catalogue of 6.7 GHz methanol masers*

M. Szymczak****, P. Wolak, A. Bartkiewicz,** and **K.M. Borkowski**

Toruń Centre for Astronomy, Nicolaus Copernicus University, Gagarina 11, 87-100 Toruń, Poland

Received 2012 April 13, accepted 2012 May 2
Published online 2012 Jul 20

Key words masers – stars: formation – radio lines: ISM – catalogues

We report the observations of 289 methanol maser sources at 6.7 GHz obtained over a two month period with the Torun 32 m telescope. The data form a catalogue of all objects north of $\delta = -22^\circ$ brighter than 7.5 Jy in the peak. The positions of sub-arcsecond accuracy are updated for 76% of the objects. We find that about one third of the sources show changes in the peak fluxes by a factor of two or more on time scales of 8.5 – 9.5 years.

1 Introduction

The class II methanol maser at 6668.519 MHz is one of the most spectacular manifestations of nascent or newly formed high-mass stars which are still embedded in their natal molecular clouds (Menten 1991). It is potentially powerful tool for investigating the environments of these objects and their distribution in the Galaxy. High-resolution imaging of the maser line enables precise measurements of proper motions and trigonometric parallaxes (e.g. Reid et al. 2009; Rygl et al. 2010).

Extensive targeted surveys of low angular resolution (a few arcmin) have resulted in a large number of detections toward IRAS selected ultra-compact HII regions (Schutte et al. 1993; van der Walt, Gaylard & MacLeod 1995; van der Walt et al. 1996; Walsh et al. 1997; Szymczak, Hrynek & Kus 2000), OH and H_2O masers (Caswell et al. 1995; Xu et al. 2008). No methanol masers were detected toward low-mass star formation sites (Minier et al. 2003). Unbiased methanol surveys of selected areas of the Galactic plane (Caswell 1996; Ellingsen et al. 1996; Szymczak et al. 2002; Pandian, Goldsmith & Deshpande 2007; Green et al. 2009, 2010; Caswell et al. 2010) proved very effective in detecting methanol sources where no clear indicators of high-mass star formation were previously known.

Majority of sources from single-dish surveys have no positions of sufficient accuracy for VLBI and multi-wavelength studies. Hence several sources have been observed with radio arrays to determine the position with a sub-arcsecond or higher accuracy (e.g. Walsh et al. 1998; Bartkiewicz et al. 2009; Caswell 2009; Cyganowski et al. 2009; Xu et al. 2009; Green et al. 2010). In many cases the data from untargeted surveys are homogeneous in sensitivity and resolutions (Ellingsen et al. 1996; Szymczak et al. 2002; Pandian et al. 2007; Green et al. 2010) but they were taken at various occasions over 9−22 months. This means that they are not entirely appropriate for variability studies.

There are several catalogues of 6.7 GHz masers based solely on the data from the literature (Xu, Zheng & Jiang 2003; Malyshev & Sobolev 2003; Pestalozzi, Minier & Booth 2005) which have some value for statistical purposes. Generally they contain highly inhomogeneous data of diverse quality and commonly taken with various instruments at very different epochs. Presently, after the recent observations by Ellingsen (2007), Pandian et al. (2007), Xu et al. (2008), Caswell et al. (2009) and Green et al. (2010), more than 1000 sources are known. In this paper we present the catalogue data for a large sample of 6.7 GHz methanol masers of the northern sky which form a database free of the above mentioned shortcomings. It is currently used as a reference for ongoing scheme of flux monitoring with the Torun 32 m telescope. Here we show a preliminary result of the maser variability on time scales of 8-10 years, whereas a detailed statistical analysis of the objects in the catalogue is postponed to a future paper.

2 Data

2.1 Selection of sources

Most of the maser sources (∼80%) in our catalogue were extracted from the Torun 32 m telescope surveys of nearly 1400 IRAS colour-selected sources (Szymczak et al. 2000) and unbiased search of the Galactic plane from l= 8° to 90°, $|b| \leq 0.^\circ 52$ of which only data for the strip of $20^\circ \leq l \leq 40^\circ$ were published (Szymczak et al. 2002).

Data for the longitude ranges of 8°−20°and 40°−90° were obtained between 2001 January and 2003 December using the same triangular grid and observational setup as reported in Szymczak et al. (2002). About 14,880 sky po-

* Table A1 and Figure B1 are also available at the CDS via http://cdsarc.u- strasbg.fr/cgi-bin/qcat?J/AN/333/634

** Corresponding author: e-mail: msz@astro.uni.torun.pl

sitions were sampled. A channel spacing in the spectra was 0.04 km s^{-1} and the velocity coverage was $\pm$90 km s^{-1}. For the galactic longitudes of 8°$-$20° and 40°$-$90° the bandwidth was centred at the local standard of rest velocity of 40 and 0 km s^{-1}, respectively. A typical 3σ sensitivity was 1.6 Jy in both targeted and blind surveys. The flux calibration uncertainty was of the order of 15% and the radial velocity determination was accurate down to 0.4 km s^{-1}. 17 out of the 128 sources detected in the regions $8^\circ \leq l \leq 20^\circ$ and $40^\circ \leq l \leq 90^\circ$ and not catalogued before 2007 are referred in Table A1 as *unpublished data from the Torun 32m dish*. Their spectra and basic parameters were published in Green et al. (2010) and Pandian et al. (2007).

The selection of 237 sources from our original list was constrained by the latitude of the Torun antenna. We have also searched the literature for the 6.7 GHz methanol maser line observations available in the NASA Astrophysics Data System (ADS) up to 1 November, 2008 and found further 50 objects north of declination -22°. All of them and another two objects (Fujisawa et al. 2008, private communication) were added to the observed list.

2.2 Observations

A sample of 289 sources was observed with the Torun 32 m radio telescope in 2008 December and 2009 January. The half-power beam width was 5′.5 at 6668.519 MHz. A dual-channel receiver was used to measure simultaneously two opposite circular polarizations. Typical system temperature was 40 K. The autocorrelator spectrometer was configured to obtain the spectra in a bandwidth of 4 MHz with channel spacing of 0.04 km s^{-1}. The spectra were taken in a frequency switching mode with about 30 min integration time. The observations were pointed on the target positions as given in the references of the first measurements.

The spectral line flux densities were continuously calibrated by measuring the receiver response to the signal from a noise diode of known temperature. The stability of the system was checked through continuum observations of 3C123 and Vir A assuming flux densities from Ott et al. (1994). The non-variable methanol source 32.745$-$0.076 (Caswell et al. 1995; Szymczak et al. 2011) was used as the secondary calibrator.

The data were reduced using the standard procedures. The spectra have a typical 3σ uncertainty of $\sim$0.6 Jy after averaging both polarizations. Hanning smoothing was only applied to noisy spectra. The flux calibration uncertainty was estimated to be of the order of $\pm$15%. The accuracy of the velocity measurements with respect to the local standard of rest was better than 0.005 km s^{-1}.

3 Catalogue and atlas

A total of 284 objects detected are listed in Table A1. Each entry of the catalogue contains the following information. Column 1 gives the source name derived from its galactic coordinates. Three significant decimal digits in each coordinate are given for the sources observed with interferometric arrays. Column 2 gives an alternative name of the source. Columns 3 and 4 give the 2000.0 right ascension and declination, respectively. Column 5 gives the velocity range of emission at the 3σ level, ΔV. Column 6 gives the velocity of peak flux, $V_{\rm p}$. Columns 7 and 8 give the peak flux density, $S_{\rm p}$ and integrated flux density, $S_{\rm i}$, respectively. Column 9 gives the reference for the first detection. Column 10 gives the reference for the coordinates. Remarks on the multiple sources unresolved with the beam and on possible confusion effect are given in column 11. Note that the coordinates of sources given in Table A1 are derived largely from the high angular resolution studies published after 2009 January when our observations were completed. However, the actual observations were pointed on the positions inferred from single dish measurements or the positions of infrared counterparts. In Sect. 4.2 we discuss the effect of position offset on the flux density estimates.

The spectra are shown in Figure B1. In 33 of the plots the emission from neighbouring sources near the edge of the antenna beam is shown. In these blended spectra the velocity ranges of the principal and confused sources are marked and their names are given if possible. For several confused sources detailed comments and references are also given in the notes to Table A1.

3.1 Galactic distribution

The galactic distribution of 284 sources in the catalogue is shown in Figure 1. For the galactic longitude higher than 50° the number of sources rapidly drops, being 19% of the sample. The distribution in the galactic latitude has a full width at half-maximum (FWHM) of 0.°39. These results are fully consistent with the trends reported previously (Pestalozzi et al. 2005; Pandian & Goldsmith 2007). The data of high angular resolution (see notes in Table A1) imply that 25 sites in the sample are actually clusters of two or more sources not resolved or barely resolved with the 32 m telescope beam. A total number of sources in the clusters is at least 68. The mean angular size of the cluster is 1′.5$\pm$0′.3. All but one cluster lay in the inner Galaxy (l <50°) and their distribution in the latitude has a FWHM of 0.°26. The extent of the emission from the clusters is usually less than 17 km s^{-1}. This suggests that the emission comes from a cluster rather than physically separated objects.

3.2 Line parameters

The extent of the emission ranges from 0.6 to 28.5 km s^{-1} and its average and median values are 7.5$\pm$0.3 km s^{-1} and 6.8 km s^{-1}, respectively. These values are similar to those reported in deep unbiased studies (Green et al. 2010; Pandian et al. 2007). The 9.621+0.196 and 133.947+1.064 are the brightest sources in the catalogue with the peak flux density of 4357 and 3275 Jy, respectively. The median values of

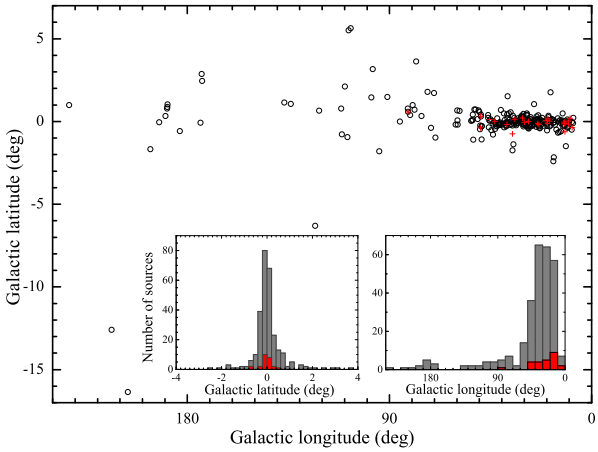

Fig. 1 Distribution of the maser sources in the longitude-latitude plane. The crosses indicate the clusters of sources. The insets show histograms of objects versus the galactic latitude and galactic longitude. Histograms for the clusters (red colour) are overlayed.

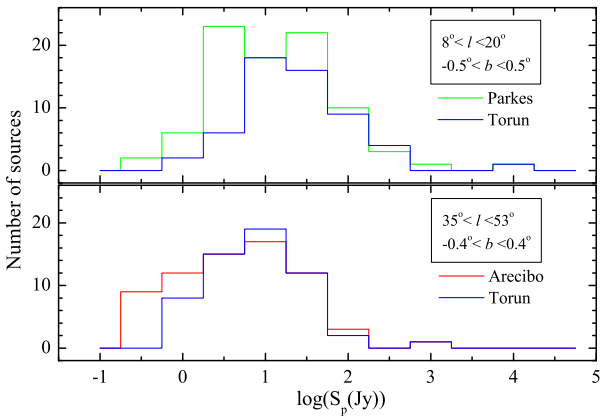

Fig. 2 Histograms of the CH_3OH maser peak flux density for sources in the present sample and two comparison samples from untargeted surveys using the Parkes telescope (Green et al. 2010, upper panel) and the Arecibo telescope (Pandian et al. 2007, lower panel). The shared areas defined by the ranges of galactic coordinates are given in insets.

peak flux density and integrated flux density are 8.7 Jy and 10 Jy km s^{-1}, respectively.

4 Discussion

4.1 Completeness of catalogue

In order to examine the completeness of the catalogue we used the Parkes and Arecibo untargeted surveys (Green et al. 2010; Pandian et al. 2007). The Parkes telescope observed the region $8^\circ \leq l \leq 20^\circ$, $|b| \leq 2^\circ$ with a 3σ limit of 0.51 Jy and spectral resolution of 0.11 km s^{-1} (Green et al. 2010). In common strip of $8^\circ \leq l \leq 20^\circ$, $|b| \leq 0\overset{\circ}{.}52$, 56 sources were found in the Torun untargeted survey with a detection threshold of 1.6 Jy, whereas with the Parkes telescope 100 objects were detected. 25 out of those 100 sources formed clusters (2-3 sources) of average size less than $2\overset{\prime}{.}3$ and they could not be well resolved with the 32 m antenna. Therefore, 86 sources were used to compare with the Torun subsample obtained with smaller angular resolution. The median values of the peak flux density of sources in the Parkes and Torun subsamples were 5.7 and 10.6 Jy, respectively. The peak flux density of objects not detected in the Torun survey ranged from 0.2 to 12 Jy and the median value was 1.9 Jy. The strongest undetected source 9.215−0.202 had S_p=11.9 Jy in the pointed Parkes observations. Figure 2 (upper panel) shows the histograms of the peak flux density for both subsamples. Despite possible effect of variability (Sect. 4.3), it suggests that all the sources of S_p >7.6 Jy within this surveyed area are included in our catalogue. This is slightly worse than the completeness limit of 5.2 Jy estimated for 20° to 40° longitude survey (Szymczak et al. 2002).

The Arecibo telescope surveyed the region $35\overset{\circ}{.}2 \leq l \leq 53\overset{\circ}{.}7$, $|b| \leq 0\overset{\circ}{.}41$ with a survey threshold of 0.27 Jy, spectral resolution of 0.14 km s^{-1} and the beam of 40″ (Pandian et al. 2007). As the Arecibo survey had angular resolution a factor of 8.2 higher than that of the Torun survey we could resolve with the 32 m telescope only 69 of their 86 sources. In this region we catalogued 57 masers. Comparison of the flux density distribution in the two subsamples (Fig. 2, lower panel) indicates that the catalogue contains all the masers with S_p >1.8 Jy detected in the Arecibo survey. This simply resulted from the inclusion of sources with S_p below the sensitivity (1.6 Jy) of our previous surveys but detected in the present observation. We conclude that the completeness of the catalogue is not uniform for the galactic longitude. Nevertheless, all maser sources brighter than 7.5 Jy in the peak are included.

4.2 Effect of pointing errors

The observations were pointed at the positions determined in the original targeted and blind surveys (Szymczak et al. 2000, 2002), which were accurate to about $0\overset{\prime}{.}5$ for the signal to noise ratio higher than 10 and less than 1′ for faint objects. Several methanol maser studies of different levels of astrometric accuracy were published after 2009 January (Bartkiewicz et al. 2009; Caswell 2009; Cyganowski et al. 2009; Green et al. 2010; Rygl et al. 2010; Xu et al. 2009) when data presented here were being gathered. There are 216 sources in the catalogue whose positions are known with an accuracy better than 1″. Fig. 3 shows the distribution of objects versus the angular separation between the position observed with the 32 m dish and that derived from astrometric measurements. The mean separation is $0\overset{\prime}{.}37 \pm 0\overset{\prime}{.}04$ and the median is $0\overset{\prime}{.}17$. Using the antenna beam pattern we estimate that in 94.9% (206/216) of the sources the position offset causes underestimation of the flux density by less than 10% that is comparable with the accuracy of flux calibration achieved in the present study. There are only 8

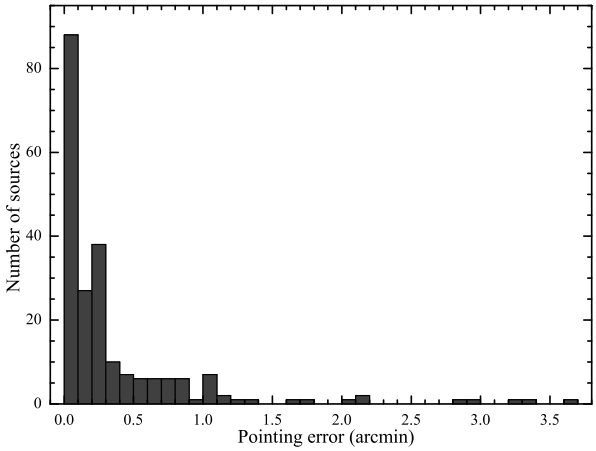

Fig. 3 Number of methanol masers as a function of angular offset between the astrometric and observed positions.

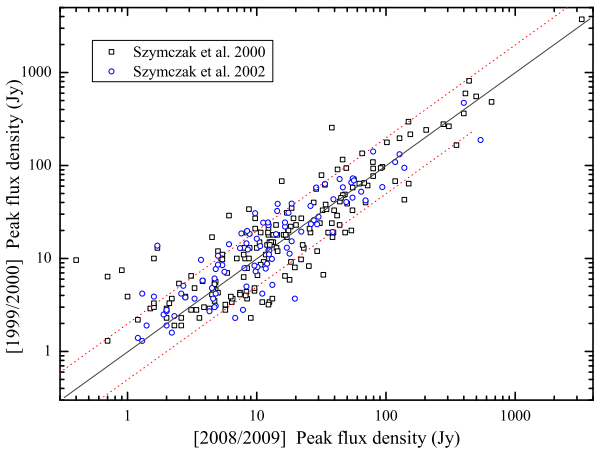

Fig. 4 Variability in source peak flux density between the epoch 1999/2000 (Szymczak et al. 2000; Szymczak et al. 2002) and the present observations (epoch 2008/2009). The straight solid line corresponds to equal fluxes, whereas the dashed lines delimit the variability of 50%.

sources whose flux density is underestimated by about 50%. All those objects are indicated in Table A1.

4.3 Variability

A majority of sources in the catalogue were first observed from 1999 January to August (E1) (Szymczak et al. 2000) and between 2000 February and October (Szymczak et al. 2002), while the observations reported here were carried out from 2008 December to 2009 January (E2). Thus, we can determine a level of variability on time scales in the range 8.5 to 9.5 years. There are 204 sources in the sample for which we have the methanol spectra taken at both epochs.

Fig. 4 shows the peak flux density at epoch 1999/2000 versus that at epoch 2008/2009. The flux density values group up well around the equal flux density line with a scatter

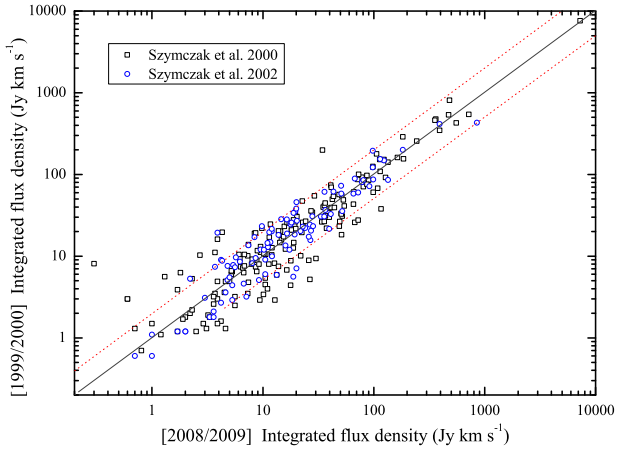

Fig. 5 Same as in Fig. 4 but for the integrated flux density.

caused by the variability. The ratio of peak flux density at the first epoch to that at the second epoch observations has the mean value of 1.12 ± 0.06. There is a wider spread of flux density for weaker sources than for stronger ones. Very likely, it is the effect of relatively larger noise variations.

Comparison of the integrated flux densities at the two epochs is shown in Fig. 5. The mean value and dispersion for the ratio of integrated flux density at the first and second epochs are 1.21 and 0.05, respectively. This dispersion is slightly less than that seen for the peak flux density.

We find that the peak flux or integrated flux densities changed by a factor of two or more in 68 sources (Table 1); 37 sources increasing and 31 sources decreasing. Our fraction of highly variable sources 33.3% (68/204) is very similar to 31.5% deduced from a sample of 54 objects monitored over a period of $\sim$4 years (Goedhart, Gaylard & van der Walt (2004), assuming that the highly variable sources have their variability index higher than 5. We notice different types of variability in our sample. For instance, the source $23.32-0.30$ exhibited a strong decrease of the peak flux while the the integrated flux density increased by a factor of 2.6. The peak flux density and the integrated flux density in the source $22.435-0.169$ increased by factors of 3.8 and 5.1, respectively, while in the source $23.82+0.38$ they decreased 2.4 and 2.7 times, respectively. A detailed investigation of individual strongly varying sources will be presented elsewhere.

High angular resolution studies of 6.7 GHz methanol masers indicate that individual spots show significant variability. For instance in the source $23.010-0.411$ about 37% of the methanol spots change their brightness by more than 50%, whereas 83% of the total spots persist on time scale of two years (Sanna et al. 2010). Further VLBI observations will be useful to understand better the properties and origin of the variability. The present catalogue can serve as a guide to select the most interesting targets.

Comparison of our old and new data reveals the disappearance of five sources (Table 2). All of them were faint

Table 1 Highly variable sources

Name	S_p(E1) (Jy)	S_p(E2)	S_i(E1) (Jy km s^{-1})	S_i(E2)	Name	S_p(E1) (Jy)	S_p(E2)	S_i(E1) (Jy km s^{-1})	S_i(E2)
10.444−0.018	9.8	22.0	23.3	48.8	30.317+0.070	11.0	5.4	19.0	8.4
10.629−0.333	3.4	6.4	2.9	12.8	30.701−0.064	43.0	138.6	27.7	72.2
10.886+0.123	4.5	9.6	8.2	12.7	30.790+0.205	19.8[a]	8.4	45.9[a]	20.1
11.497−1.485	116.0	46.2	178.8	105.7	30.816−0.052	4.3	7.4	4.4	17.8
12.904−0.031	8.3	25.3	9.4	30.1	30.97−0.14	5.9	17.9	8.9	25.9
13.179+0.061	6.4	0.7	3.0	0.6	31.064+0.093	6.5	16.5	4.0	11.0
13.713−0.083	3.4	12.5	3.5	7.3	32.992+0.034	27.0	9.7	22.0	9.8
14.101+0.087	135.0	65.3	152.3	112.9	34.751−0.093	9.7[a]	3.7	9.0[a]	4.2
14.604+0.017	2.9	1.5	5.3	2.3	35.197−0.743	64.0	150.	91.8	127.8
15.034−0.677	19.0	48.2	8.8	17.9	36.115+0.552	19.0	39.2	32.7	51.0
17.021−2.403	3.7	6.5	2.9	9.4	37.030−0.039	7.3[a]	9.8	7.1[a]	20.1
18.874+0.053	3.7	8.4	1.6	4.2	37.546−0.112	5.7	3.8	19.7	4.3
19.365−0.030	6.7	32.7	10.1	21.9	37.598+0.425	24.3[a]	11.2	28.3[a]	14.6
19.884−0.534	2.3	9.0	1.3	4.6	38.038−0.300	18.6[a]	7.6	21.6[a]	12.0
21.407−0.254	3.7	13.2	5.9	13.3	38.916−0.353	5.4	2.5	3.9	1.7
22.357+0.066	12.0	14.5	6.8	16.4	41.226−0.197	3.2	5.7	3.4	10.1
22.435−0.169	3.2	12.3	5.2	26.5	43.796−0.127	79.0	31.6	54.7	29.1
23.010−0.411	188.5[a]	538.	431.3[a]	849.9	43.890−0.784	34.0	8.7	25.5	17.3
23.207−0.377	12.0	29.3	43.4	65.6	50.03+0.58	6.5	3.1	6.6	5.2
23.257−0.241	4.4	8.3	4.5	10.5	53.036+0.113	3.3	1.6	1.3	0.7
23.32−0.30	2.2	1.2	1.5	3.9	58.77+0.64	2.8	5.7	4.8	7.4
23.389+0.185	17.0	38.5	31.0	52.0	60.57−0.19	4.1	7.4	1.2	2.5
23.481+0.092	12.0	5.0	9.2	8.0	73.06+1.80	10.0	1.6	6.3	1.8
23.82+0.38	9.6	0.4	8.1	0.3	78.122+3.633	38.0	34.1	18.3	51.1
24.493−0.039	29.0	6.1	24.6	11.7	108.184+5.519	91.0	42.1	47.4	22.6
24.68−0.16	3.5	4.7	2.5	5.6	108.76−0.99	2.8	3.4	1.3	3.1
24.850+0.087	13.0	1.7	16.1	3.9	111.26−0.77	4.0	8.2	6.5	8.8
25.411+0.105	8.0	19.7	12.6	18.8	136.84+1.15	21.0	9.7	11.1	3.7
25.80−0.16	20.0	53.9	26.0	67.3	173.482+2.446	256.0	38.1	198.6	34.5
26.60−0.22	19.0	8.3	20.4	13.8	173.70+2.89	7.5	0.9	3.0	0.6
27.220+0.260	2.8[a]	7.8	3.2[a]	7.1	183.35−0.58	18.0	13.4	19.3	8.6
28.39+0.08	3.4	11.0	8.0	9.2	189.77+0.34	17.0	4.5	10.3	2.7
28.70+0.40	4.2[a]	1.3	0.6[a]	0.7	196.454−1.677	68.0	15.6	37.9	116.0
30.30−0.20	3.9	1.0	5.6	1.3	213.705−12.597	166.0	350.4	155.7	184.9

[a] - Szymczak et al. 2002

Table 2 Disappeared and appeared maser sources.

Name	Other name	First epoch S_p(Jy) [S_i(Jy km s^{-1})]	Second epoch S_p(Jy) [S_i(Jy km s^{-1})]
14.44−0.06	IRAS18141−1626	3.0[1.0]	<0.65[<0.2]
15.08−0.12	IRAS18155−1554	3.1[1.1]	<0.60[<0.2]
26.64+0.02	IRAS18372−0537	5.9[2.5]	<0.60[<0.2]
30.59−0.13		2.2[0.7]	<0.55[<0.2]
43.18−0.52	IRAS19097+0847	5.5[3.1]	<0.60[<0.2]
52.23+0.73	IRAS19227+1721[a]	<1.8[<0.5]	4.2[2.9]
107.29+5.64	IRAS22198+6336[a]	<1.9[<0.5]	1.5[0.9]

[a] Fujisawa et al. (2008, private communication)

($S_{\rm p}$ <6 Jy) at the first epoch and were not re-detected with a 3σ sensitivity of 0.55−0.65 Jy at the second epoch. This suggests that only ∼2% of sources in the original sample disappeared after 9.5 years. We note that two sources (Table 2) in the catalogue were detected by Fujisawa et al. (2008, private communication) who re-observed the non-detections of Szymczak et al. (2000) survey.

5 Summary

The paper presents observations of the 6.7 GHz methanol maser emission towards 289 targets. 284 sources were detected of which 25 sources form clusters unresolved with the 5.′5 beam. A comparison of an earlier epoch data and the present survey reveals that 33% of the sources show significant variability (more than 50%) on time scale of 8.5 or 9.5 years. The catalogue can be the potential to become a reference for further studies of variability. Since the catalogue gives the interferometric position for about 76% of the sources it will be useful database for future VLBI measurements of the proper motions and trigonometric parallaxes.

Acknowledgements. We thank G. Fuller for communicating the MERLIN astrometric observations prior to publication, K. Fujisawa and K. Sugiyama for allowing us to use their methanol maser data observed with the Yamaguchi 32m radio telescope before publication. We have made use of NASA's Astrophysics Data System Bibliographic Services and the SIMBAD database operated at CDS, Strasbourg, France. The work was supported by the Polish Ministry of Science and Higher Education through grant N N203 386937.

References

Bartkiewicz, A., Szymczak, M., van Langevelde, H.J., Richards, A.M.S, Pihlström, Y.M.: 2009, A&A 502, 155
Caswell, J., Vaile, R., Ellingsen, S., Whiteoak, J., Norris, R.: 1995, MNRAS 272, 96
Caswell, J.L.: 1996, MNRAS 279, 79
Caswell, J.L.: 2009, PASA 26, 454
Caswell, J.L., Fuller, G.A., Green, J.A., et al.: 2010, MNRAS 404, 1029
Cyganowski, C.J., Brogan, C.L., Hunter, T.R., Churchwell, E.: 2009, ApJ 702, 1615
Ellingsen, S., von Bibra, M., McCulloch, P., Norris, R.P., Deshpande, A.A., Phillips, C.J.: 1996, MNRAS 280, 378
Ellingsen, S. P.: 2007, MNRAS 377, 571
Etoka, S., Cohen, R.J., Gray, M.D.: 2005, MNRAS 360, 116
Gaylard, M., MacLeod, G.: 1993, MNRAS 262, 43
Goedhart, S., Gaylard, M.J., van der Walt, D.J.: 2004, MNRAS 355, 553
Goddi, C., Moscadelli, L., Sanna, A., Cesaroni, R., Minier, V.: 2007, A&A 461, 1027
Green, J.A., Caswell, J.L., Fuller, G.A., et al.: 2009, MNRAS 392, 783
Green, J.A., Caswell, J.L., Fuller, G.A., et al.: 2010, MNRAS 409, 913
Harvey-Smith, L., Soria-Ruiz, R., Duarte-Cabral, A., Cohen, R.J.: 2008, MNRAS 384, 719
MacLeod, G.C., Gaylard, M.J.: 1992, MNRAS 256, 519
Malyshev, A.V., Sobolev, A.M.: 2003, A&ATr 22, 1
Menten, K.M.: 1991, ApJ 380, L75
Minier, V., Booth, R.S., Conway, J.E.: 2000, A&A 362, 1093
Minier, V., Conway, J.E., Booth, R.S.: 2001, A&A 369, 278
Minier, V., Ellingsen, S.P., Norris, R.P., Booth, R.S.: 2003, A&A 403, 1095
Moscadelli, L., Goddi, C., Cesaroni, R., Beltrán, M.T., Furuya, R.S.: 2007, A&A 472, 867
Ott, M., Witzel, A., Quirrenbach, A., Krichbaum, T.P., Standke, K.J., Schalinski, C.J., Hummel, C.A.: 1994, A&A, 284, 331
Pandian, J.D., Goldsmith, P.F., & Deshpande, A.A.: 2007, ApJ 656, 255
Pandian, J.D., Goldsmith, P.F.: 2007, ApJ 699, 435
Pandian, J.D., Momjian, E., Xu, Y., Menten, K.M., Goldsmith, P.F.: 2011, ApJ 730, 55
Pestalozzi M.R., Minier V. Booth, R.S.: 2005, A&A 432, 737
Reid, M.J., Menten, K.M., Zheng, X.W., et al.: 2009, ApJ 700, 137
Rygl, K.L.J., Brunthaler, A., Reid, M.J., Menten, K.M., van Langevelde, H.J., Xu, Y.: 2010, A&A 511, A2
Sanna, A., Moscadelli, L., Cesaroni, R., Tarchi, A., Furuya, R.S., Goddi, C.: 2010, A&A 517, 78
Slysh, V., Val'tts, I., Kalenskii, S.: 1999, A&AS 134, 115
Schutte, A.J., van der Walt, D.J., Gaylard, M.J., MacLeod, G.C.: 1993, MNRAS 261, 783
Sridharan, T.K., Beuther, H., Schilke, P., Menten, K.M., Wyrowski, F.: 2002, ApJ 566, 931
Sugiyama, K., Fujisawa, K., Doi, A., Honma, M., Isono, Y., Kobayashi, H., Mochizuki, N., Murata, Y.: 2008, PASJ 60, 23
Szymczak, M., Hrynek, G., Kus, A.: 2000, A&AS 143, 269
Szymczak, M., Kus, A., Hrynek, G., Kepa, A., Pazderski, E.: 2002, A&A 392, 277
Szymczak, M., Wolak, P., Bartkiewicz, A., van Langevelde, H.J.: 2011, A&A, 531, L3
van der Walt, D., Gaylard, M., MacLeod, G.: 1995, A&AS 110, 81
van der Walt, D., Retief, S., Gaylard, M., MacLeod, G.: 1996, MNRAS 282, 1085
Walsh, A., Hylard, A., Robinson, G., Burton, M.: 1997, MNRAS 291, 261
Walsh, A.J., Burton, M.G., Hyland, A.R., Robinson G.: 1998, MNRAS 301, 640
Xu, Y., Zheng, X.W., Jiang, D.R.: 2003, ChJAA 3, 49
Xu, Y., Li, J.J., Hachisuka, K., Pandian, J.D., Menten, K.M., Henkel, C.: 2008, A&A 485, 729
Xu, Y., Voronkov, M.A., Pandian, J.D., Li, J.J., Sobolev, A.M., Brunthaler, A., Ritter, B., Menten, K.M.: 2009, A&A 507, 1117

A Catalogue

Table A1: Catalogue of 6.7 GHz methanol masers

Name	Other name	RA(2000) (h m s)	Dec(2000) (° ′ ″)	ΔV (km s^{-1})	$V_{\rm p}$ (km s^{-1})	$S_{\rm p}$ (Jy)	$S_{\rm i}$ (Jy km s^{-1})	References det.	References pos.	Notes
8.317−0.096		18 04 36.02	−21 48 19.6	+44.6;+48.7	+46.90	2.0	2.7	2, 3	2	
8.683−0.368		18 06 23.49	−21 37 10.2	+36.0;+45.8	+43.09	124.3	124.0	4	2	1
8.832−0.028		18 05 25.66	−21 19 25.5	−6.3;+5.7	−3.87	125.8	308.1	2, 5	3	
8.872−0.493		18 07 15.32	−21 30 54.4	+22.7;+26.8	+23.22	31.6	27.7	2, 5	3	
9.621+0.196		18 06 14.67	−20 31 32.4	−4.3;+9.1	+1.25	4357.0	1854.0	4	2	2
9.986−0.028		18 07 50.12	−20 18 56.5	+40.5;+51.6	+42.21	50.7	66.1	1	4	
10.320−0.259		18 09 23.30	−20 08 06.9	+35.2;+40.7	+39.03	8.0	10.8	6	4	3
10.323−0.160		18 09 01.46	−20 05 07.8	+3.2;+20.4	+11.53	90.4	162.2	1	2	4
10.444−0.018		18 08 44.88	−19 54 38.2	+67.6;+78.7	+73.30	22.0	48.8	4	2	5
10.472+0.027		18 08 38.20	−19 51 50.1	+57.7;+78.5	+75.00	35.7	108.3	4	2	6
10.627−0.384		18 10 29.22	−19 55 41.1	−6.0;+7.6	+4.48	4.1	7.0	7	4	7
10.629−0.333		18 10 17.98	−19 54 04.8	−13.5;+1.0	−8.06	6.4	12.8	7	4	8
10.886+0.123		18 09 07.98	−19 27 21.8	+13.3;+22.0	+17.12	9.6	12.7	8	2	
10.958+0.022		18 09 39.32	−19 26 28.0	+23.5;+25.3	+24.47	13.4	10.6	1	4	
11.109−0.114		18 10 28.25	−19 22 29.1	+22.8;+34.2	+23.90	6.9	11.2	2, 9	2	54
11.497−1.485		18 16 22.13	−19 41 27.1	+4.4;+17.3	+6.59	46.2	105.7	1	4	
11.904−0.141		18 12 11.44	−18 41 28.6	+39.5;+44.2	+42.79	48.1	54.1	7	4	9
11.936−0.616		18 14 00.89	−18 53 26.6	+29.8;+44.3	+32.21	43.9	66.2	7	4	10
11.992−0.272		18 12 51.19	−18 40 38.4	+56.0;+60.9	+59.77	2.0	1.7	10	2	
12.025−0.031		18 12 01.86	−18 31 55.7	+104.9;+112.8	+108.22	79.6	86.7	7	4	
12.199−0.034		18 12 23.44	−18 22 50.9	+48.0;+57.2	+49.28	11.3	14.7	8	4	11
12.209−0.102		18 12 39.92	−18 24 17.9	+16.0;+22.0	+19.67	8.4	14.4	7	4	12
12.265−0.051		18 12 35.40	−18 19 52.3	+58.0;+71.0	+68.29	2.4	5.9	2, 11	4	13
12.526+0.016		18 12 52.04	−18 04 13.6	+39.3;+43.4	+42.64	4.0	3.5	2, 3	2	
12.625−0.017		18 13 11.30	−17 59 57.6	+20.9;+28.0	+21.54	14.2	15.6	6	4	14
12.681−0.182		18 13 54.75	−18 01 46.6	+50.2;+61.6	+58.35	306.0	717.9	7	4	
12.889+0.489		18 11 51.40	−17 31 29.6	+26.8;+40.2	+39.18	72.0	90.1	7	4	
12.904−0.031		18 13 48.27	−17 45 38.8	+57.6;+60.4	+58.85	25.3	30.1	8	2	54, 15
12.909−0.260		18 14 39.53	−17 52 00.0	+35.1;+41.9	+39.80	204.4	244.4	7	4	
13.179+0.061		18 14 00.96	−17 28 32.5	+46.0;+49.5	+46.37	0.7	0.6	8	2	
13.657−0.599		18 17 24.27	−17 22 12.5	+46.3;+53.0	+51.11	32.3	42.2	8	4	
13.713−0.083		18 15 36.99	−17 04 31.8	+42.8;+52.9	+43.53	12.5	7.3	8	2	
14.101+0.087		18 15 45.80	−16 39 09.7	+4.2;+16.9	+15.30	65.3	112.9	6	3	
14.33−0.64		18 18 53.8	−16 47 46.6	+21.4;+23.7	+22.64	0.6	0.6	10	5	
14.604+0.017		18 17 01.14	−16 14 38.0	+21.8;+35.3	+24.62	1.5	2.3	10	1	
15.034−0.677		18 20 24.78	−16 11 34.6	+20.8;+23.7	+21.27	48.2	17.9	7	4	
15.094+0.192		18 17 20.82	−15 43 46.5	+22.3;+26.2	+25.72	13.6	8.8	2, 3	2	
15.665−0.499		18 20 59.75	−15 33 10.0	−4.8;−2.3	−3.00	39.6	19.0	8	2	
16.302−0.196		18 21 07.83	−14 50 54.6	+49.3;+52.7	+51.85	8.1	7.3	8	2	54
16.585−0.051		18 21 09.13	−14 31 48.5	+56.4;+69.2	+62.06	30.8	39.5	7	2	
16.831+0.079		18 21 09.53	−14 15 08.6	+58.1;+68.9	+58.72	2.7	5.3	2, 3	2	54
16.864−2.159		18 29 24.42	−15 16 04.5	+14.3;+19.2	+14.89	20.1	14.2	4	2	
17.021−2.403		18 30 36.30	−15 14 28.5	+16.7;+24.7	+23.54	6.5	9.4	8	2	
17.029−0.071		18 22 05.21	−14 08 51.0	+90.6;+94.1	+91.33	0.7	0.8	8	2	
17.638+0.157		18 22 26.30	−13 30 12.1	+20.3;+21.2	+20.71	17.4	4.6	12	4	
18.073+0.077		18 23 33.98	−13 09 25.0	+44.3;+59.0	+55.54	6.3	8.8	8	2	
18.159+0.094		18 23 40.18	−13 04 21.0	+54.3;+59.4	+58.27	7.9	6.3	8	2	
18.262−0.244		18 25 05.70	−13 08 23.2	+72.5;+80.4	+75.71	23.1	34.0	8	2	54
18.341+1.768		18 17 58.13	−12 07 24.8	+26.8;+31.7	+27.99	67.8	34.9	13	2	
18.460−0.004		18 24 36.34	−12 51 08.6	+46.9;+49.8	+49.37	22.6	13.8	7	2	
18.667+0.025		18 24 53.78	−12 39 20.8	+76.1;+82.8	+78.70	18.3	27.9	8	6	16
18.834−0.300		18 26 23.66	−12 39 38.0	+38.5;+43.2	+41.11	3.6	3.2	6	2	
18.874+0.053		18 25 11.34	−12 27 36.8	+37.7;+39.7	+38.63	8.4	4.2	8	2	
19.009−0.029		18 25 44.77	−12 22 46.0	+53.4;+60.8	+55.19	9.1	13.6	9	6	54
19.249+0.267		18 25 08.02	−12 01 42.2	+12.5;+25.0	+20.38	1.9	3.5	2, 3	2	

Table A1: continued.

Name	Other name	RA(2000)	Dec(2000)	ΔV	$V_{\rm p}$	$S_{\rm p}$	$S_{\rm i}$	References		Notes
19.267+0.349		18 24 52.38	−11 58 28.2	+12.8;+16.8	+16.19	3.3	2.4	2, 3	2	
19.365−0.030		18 26 25.78	−12 03 53.3	+24.3;+30.1	+25.22	32.7	21.9	10	6	
19.472+0.170		18 25 54.70	−11 52 34.6	+13.0;+27.1	+21.65	10.5	18.1	7	4	17
19.496+0.115		18 26 09.16	−11 52 51.7	+120.4;+122.0	+121.13	3.7	2.0	2, 11	4	54
19.612−0.134		18 27 16.52	−11 53 38.2	+49.3;+60.6	+56.46	10.7	11.3	4	2	18
19.701−0.267		18 27 55.52	−11 52 40.3	+41.6;+46.3	+43.82	8.7	9.5	8	2	
19.755−0.128		18 27 31.66	−11 45 55.0	+116.0;+124.2	+122.96	4.1	2.0	14	2	
19.884−0.534		18 29 14.37	−11 50 23.0	+46.1;+47.9	+46.73	9.0	4.6	8	2	
20.085−0.133		18 28 10.23	−11 28 31.1	+42.3;+44.0	+43.33	2.2	1.0	7	1	
20.237+0.065		18 27 44.56	−11 14 54.2	+68.0;+77.8	+71.74	49.2	41.0	7	4	19
21.407−0.254		18 31 06.338	−10 21 37.41	+85.4;+95.3	+88.93	13.2	13.3	8	7	
21.563−0.033		18 30 36.07	−10 07 10.9	+109.4;+120.4	+117.17	12.0	16.0	8	8	
21.882+0.013		18 31 02.17	−09 48 56.5	+16.8;+21.8	+20.21	4.3	3.3	7	1	
22.039+0.222		18 30 34.70	−09 34 47.0	+45.2;+54.8	+53.22	4.7	10.5	8	6	
22.335−0.155		18 32 29.407	−09 29 29.68	+25.0;+39.4	+35.56	30.0	24.1	15	7	20
22.357+0.066		18 31 44.120	−09 22 12.31	+79.3;+88.9	+80.12	14.5	16.4	1	7	
22.435−0.169		18 32 43.82	−09 24 33.2	+22.1;+40.2	+29.51	12.3	26.5	4	4	
23.010−0.411		18 34 40.29	−09 00 38.1	+69.2;+83.7	+74.71	538.0	849.9	7	3	
23.207−0.377		18 34 55.212	−08 49 11.89	+73.3;+85.5	+81.60	29.3	65.6	8	7	
23.257−0.241		18 34 31.26	−08 42 47.2	+59.1;+66.1	+64.09	8.3	10.5	1	1	
23.32−0.30		18 34 50.7	−08 41 20.	+73.6;+83.0	+82.66	1.2	3.9	8	5	
23.389+0.185		18 33 14.325	−08 23 57.47	+71.9;+77.6	+75.30	38.5	52.0	8	7	
23.437−0.184		18 34 39.25	−08 31 38.5	+101.0;+108.0	+102.90	69.5	78.4	7	4	21
23.481+0.092		18 33 44.75	−08 21 37.8	+81.2;+93.0	+86.99	5.0	8.0	1	1	
23.657−0.127		18 34 51.565	−08 18 21.30	+75.7;+87.8	+82.38	11.7	39.6	15	7	
23.707−0.198		18 35 12.366	−08 17 39.36	+72.6;+82.7	+76.41	18.4	49.4	1	7	
23.82+0.38		18 33 19.5	−07 55 38.1	+75.7;+76.7	+76.21	0.4	0.3	8	5	
23.90+0.08		18 34 34.6	−07 59 42.5	+35.2;+45.3	+44.90	1.1	1.2	16	13	
23.966−0.109		18 35 22.215	−08 01 22.47	+64.0;+72.6	+70.83	17.1	12.1	8	7	22
24.148−0.009		18 35 20.943	−07 48 55.67	+16.2;+19.7	+17.40	27.6	19.3	8	7	
24.329+0.144		18 35 08.14	−07 35 04.0	+109.2;+120.2	+110.29	4.8	8.6	7	3	
24.493−0.039		18 36 05.83	−07 31 20.6	+107.0;+116.0	+114.97	6.1	11.7	13	4	
24.541+0.312		18 34 55.721	−07 19 06.65	+104.0;+110.3	+105.52	12.5	22.9	8	7	
24.634−0.324		18 37 22.713	−07 31 42.14	+34.2;+46.4	+35.47	6.8	5.3	15	7	
24.68−0.16		18 36 51.4	−07 24 43.3	+111.1;+116.9	+116.03	4.7	5.6	6	5	
24.790+0.083		18 36 12.563	−07 12 10.79	+102.1;+116.7	+113.33	93.5	134.5	7	8, 9	
24.850+0.087		18 36 18.40	−07 08 53.1	+107.3;+115.5	+110.10	1.7	3.9	8	1	23
24.943+0.074		18 36 31.55	−07 04 16.8	+45.1;+53.7	+53.19	4.8	5.3	15	6	24
25.38−0.18		18 38 14.5	−06 48 02.0	+56.7;+62.8	+58.10	4.6	5.2	16	5	
25.39+0.03		18 37 30.28	−06 41 17.7	+94.1;+97.5	+95.36	0.8	1.2	17	5	
25.411+0.105		18 37 16.921	−06 38 30.50	+92.8;+100.0	+97.19	19.7	18.8	13	7	
25.653+1.046		18 34 21.99	−05 59 38.6	+36.7;+43.9	+41.76	101.5	41.4	13	1	
25.709+0.044		18 38 03.15	−06 24 15.8	+88.8;+103.2	+95.57	399.6	392.8	10	1	
25.80−0.16		18 38 56.4	−06 24 52.7	+84.1;+100.0	+91.59	53.9	67.3	1	5	
26.53−0.27		18 40 40.2	−05 49 12.8	+102.0;+115.3	+104.23	5.5	9.4	17	5	
26.598−0.024		18 39 55.926	−05 38 44.64	+17.8;+26.4	+24.82	8.8	9.5	8	7	
26.60−0.22		18 40 38.5	−05 44 01.3	+102.2;+115.5	+103.29	8.3	13.8	13	13	
27.01−0.04		18 40 44.8	−05 17 09.1	−22.3;−17.5	−21.09	1.1	1.5	18	10	
27.220+0.260		18 40 03.72	−04 57 45.6	+7.4;+10.8	+9.19	7.8	7.1	15	3	
27.221+0.136		18 40 30.546	−05 01 05.39	+105.0;+121.2	+118.81	13.1	21.8	15	7	
27.28+0.14		18 40 35.28	−04 57 44.7	+33.5;+36.4	+34.76	12.3	7.4	6	5	
27.365−0.166		18 41 51.06	−05 01 42.8	+97.3;+102.1	+99.74	14.1	27.2	7	3	
27.784+0.057		18 41 49.58	−04 33 13.8	+108.2;+113.4	+111.87	2.3	3.6	8	8	
27.78−0.26		18 42 56.3	−04 41 58.9	+96.4;+106.5	+98.18	3.9	2.9	8	13	
27.83−0.24		18 42 58.5	−04 38 47.3	+19.2;+20.5	+20.13	0.7	0.4	16	5	
28.011−0.426		18 43 57.97	−04 34 24.1	+15.6;+28.3	+16.89	3.3	4.8	15	8	
28.146−0.005		18 42 42.59	−04 15 36.5	+97.2;+104.9	+101.13	28.8	20.3	4	4	25
28.201−0.049		18 42 58.08	−04 13 56.2	+94.0;+101.8	+97.27	1.9	4.2	7	4	
28.282−0.359		18 44 13.26	−04 18 04.8	+40.5;+42.3	+41.33	3.5	2.6	1	6	

Table A1: continued.

Name	Other name	RA(2000)	Dec(2000)	ΔV	$V_{\rm p}$	$S_{\rm p}$	$S_{\rm i}$	References		Notes
28.305−0.388		18 44 22.03	−04 17 38.3	+79.6;+94.1	+81.78	33.7	43.2	1	1	
28.39+0.08		18 42 52.6	−04 00 12.5	+68.2;+82.3	+71.42	11.0	9.2	8	5	
28.53+0.13		18 42 56.5	−03 51 21.5	+23.8;+40.0	+39.56	1.3	1.7	15	5	
28.70+0.40		18 42 16.3	−03 34 50.5	+92.7;+94.5	+94.10	1.3	0.7	15	11	
28.817+0.365		18 42 37.348	−03 29 40.92	+86.3;+93.3	+90.71	5.6	11.1	15	7	
28.832−0.253		18 44 51.08	−03 45 48.5	+79.4;+92.7	+91.80	55.2	98.0	7	6	
28.84+0.49		18 42 12.5	−03 24 46.4	+79.8;+89.1	+83.26	2.0	3.6	15	12	
28.848−0.228		18 44 47.46	−03 44 17.2	+99.5;+103.6	+102.76	1.4	2.0	15	6	
28.86+0.07		18 43 45.1	−03 35 29.0	+104.3;+105.6	+104.87	0.5	0.3	4	5	
29.32−0.16		18 45 25.1	−03 17 17.0	+39.9;+49.5	+48.84	2.0	3.0	15	13	26
29.863−0.044		18 45 59.57	−02 45 04.4	+95.1;+105.2	+101.37	64.3	91.4	4	3	
29.955−0.016		18 46 03.63	−02 39 21.1	+94.8;+106.5	+95.90	127.1	182.6	7	1	27
29.978−0.048		18 46 12.96	−02 39 01.4	+102.1;+106.3	+103.44	26.2	33.4	4	8	28
30.199−0.169		18 47 03.07	−02 30 33.6	+100.6;+114.4	+108.47	12.3	35.8	4	3	29
30.225−0.180		18 47 08.30	−02 29 27.1	+102.6;+114.5	+113.18	10.6	26.8	4	3	30
30.30−0.20		18 47 21.5	−02 26 03.7	+110.8;+114.3	+113.07	1.0	1.3	8	13	
30.317+0.070		18 46 25.026	−02 17 40.75	+32.0;+38.2	+36.14	5.4	8.4	8	7	31
30.400−0.296		18 47 52.300	−02 23 16.05	+97.6;+105.8	+98.17	2.7	5.4	15	7	
30.42+0.46		18 45 12.76	−02 01 10.4	+5.3;+13.7	+7.36	1.2	1.5	14	5	
30.520+0.097		18 46 41.37	−02 06 07.6	+40.2;+48.8	+43.06	3.3	5.2	7	1	
30.53+0.02		18 46 59.4	−02 07 25.5	+40.6;+54.8	+52.82	0.8	1.5	11	5	
30.701−0.064		18 47 35.65	−02 00 53.4	+85.4;+90.2	+88.20	138.6	72.2	7	1	32
30.757−0.048		18 47 38.57	−01 57 26.4	+88.4;+94.0	+91.67	43.7	50.8	7	1	33
30.781+0.231		18 46 41.49	−01 48 32.1	+47.3;+49.2	+48.89	26.0	12.0	7	1	
30.790+0.205		18 46 48.07	−01 48 45.9	+84.2;+90.0	+84.50	8.4	20.1	4	1	34
30.816−0.052		18 47 45.83	−01 54 24.0	+98.8;+110.2	+101.39	7.4	17.8	7	1	35
30.818+0.273		18 46 36.58	−01 45 22.4	+99.7;+105.2	+104.85	1.6	2.2	7	1	36
30.899+0.162		18 47 09.13	−01 44 08.8	+98.4;+111.7	+101.76	55.0	98.6	1	3	
30.97−0.14		18 48 21.99	−01 48 30.7	+73.6;+80.3	+77.79	17.9	25.9	15	5	
31.047+0.356		18 46 43.855	−01 30 54.15	+77.7;+83.2	+81.06	4.6	6.2	8	7	
31.064+0.093		18 47 41.96	−01 37 12.5	+15.2;+20.3	+16.47	16.5	11.0	1	1	
31.156+0.045		18 48 02.347	−01 33 35.09	+40.2;+48.2	+40.81	2.0	2.0	8	7	
31.276+0.070		18 48 10.02	−01 26 31.6	+102.1;+113.4	+110.2	56.4	123.7	7	1	
31.414+0.309		18 47 34.11	−01 12 33.8	+91.3;+105.8	+95.78	12.4	36.6	1	1	
31.581+0.077		18 48 41.941	−01 10 02.53	+95.0;+100.3	+98.84	4.8	6.7	8	7	
32.04+0.06		18 49 36.6	−00 45 45.6	+91.7;+102.3	+92.79	79.4	97.7	13	13	
32.12+0.09		18 49 37.8	−00 41 00.2	+90.5;+103.8	+92.79	25.6	29.7	6	5	37
32.745−0.076		18 51 21.99	−00 12 02.8	+28.0;+39.4	+38.44	46.4	80.6	7	8	
32.80+0.19		18 50 31.0	−00 01 56.6	+25.2;+27.9	+27.38	1.4	1.4	16	5	
32.992+0.034		18 51 25.583	+00 04 08.33	+89.5;+92.7	+91.87	9.7	9.8	13	7	
33.09−0.07		18 51 59.4	+00 06 34.2	+94.5;+106.4	+103.85	12.2	19.6	4	13	
33.13−0.09		18 52 07.9	+00 08 12.0	+70.8;+80.7	+73.18	10.0	11.4	7	13	
33.39+0.01		18 52 14.5	+00 24 58.1	+96.6;+107.8	+105.17	17.6	36.0	6	13	
33.641−0.228		18 53 32.563	+00 31 39.18	+56.7;+64.2	+60.26	117.9	114.1	15	7	
33.74−0.15		18 53 26.9	+00 39 01.0	+52.8;+54.7	+54.15	1.2	1.0	15	12	38
33.85+0.02		18 53 03.1	+00 49 37.4	+59.7;+64.7	+63.93	4.7	4.6	15	13	
33.980−0.019		18 53 25.018	+00 55 25.98	+58.5;+66.0	+59.00	2.8	3.7	8	7	
34.10+0.02		18 53 29.8	+01 02 38.2	+54.5;+61.9	+56.01	4.5	5.0	15	13	
34.255+0.139		18 53 21.44	+01 14 26.0	+54.5;+62.4	+57.56	14.4	18.1	7	8	39
34.394+0.221		18 53 19.07	+01 24 05.9	+55.2;+63.1	+55.63	22.1	16.5	1	8	
34.751−0.093		18 55 05.223	+01 34 36.26	+51.6;+53.5	+52.91	3.7	4.2	15	7	
34.804−1.38		18 59 46.2	+01 01 38.1	+43.0;+49.1	+46.92	17.6	38.9	13	5	
35.02+0.350		18 54 00.66	+02 01 19.3	+41.1;+46.8	+44.34	18.6	18.9	7	6	
35.197−0.743		18 58 13.05	+01 40 35.7	+25.8;+34.2	+28.50	150.0	127.8	7	3	40
35.20−1.74		19 01 46.7	+01 13 19.6	+39.4;+45.7	+44.45	410.7	472.4	7	5	
35.247−0.237		18 56 30.388	+01 57 08.88	+71.2;+73.0	+72.36	1.6	0.9	19	14	
35.40+0.03		18 55 50.8	+02 12 25.5	+88.5;+90.0	+89.07	0.8	0.7	19	13	
35.793−0.175		18 57 16.894	+02 27 57.91	+58.2;+63.2	+60.72	16.5	20.0	15	7	
36.115+0.552		18 55 16.793	+03 05 05.41	+69.6;+84.7	+73.05	39.2	51.0	8	7	

Table A1: continued.

Name	Other name	RA(2000)	Dec(2000)	ΔV	$V_{\rm p}$	$S_{\rm p}$	$S_{\rm i}$	References		Notes
36.634−0.203		18 58 55.236	+03 12 04.72	+77.0;+79.4	+77.33	1.1	0.6	19	14	
36.705+0.096		18 57 59.123	+03 24 06.11	+52.3;+62.6	+53.02	5.0	5.7	15	7	
36.918+0.483		18 56 59.786	+03 46 03.60	−36.3;−35.5	−35.83	1.2	0.8	19	14	
37.030−0.039		18 59 03.642	+03 37 45.09	+77.7;+85.9	+80.18	9.8	20.1	15	7	41
37.43+1.52		18 54 14.5	+04 41 40.5	+40.0;+51.7	+41.12	278.0	163.1	1	5	
37.479−0.105		19 00 07.145	+03 59 53.35	+53.6;+63.2	+54.67	8.5	27.9	15	7	
37.546−0.112		19 00 16.056	+04 03 16.09	+49.2;+53.0	+49.88	3.8	4.3	19	14	42
37.554+0.201		18 59 09.985	+04 12 15.54	+78.8;+88.2	+83.64	10.1	10.2	6	14	
37.598+0.425		18 58 26.798	+04 20 45.46	+84.7;+92.9	+86.98	11.2	14.6	15	7	
37.753−0.189		19 00 55.421	+04 12 12.56	+54.3;+65.7	+54.62	1.4	1.9	19	14	43
38.038−0.300		19 01 50.469	+04 24 18.96	+54.6;+63.1	+58.13	7.6	12.0	15	7	
38.119−0.229		19 01 44.152	+04 30 37.42	+66.5;+79.7	+70.39	2.6	5.6	8	14	
38.203−0.067		19 01 18.732	+04 39 34.29	+77.9;+85.3	+84.24	9.6	17.4	15	7	
38.255−0.200		19 01 52.956	+04 38 39.47	+64.5;+73.3	+73.11	1.0	1.5	19	14	
38.258−0.073		19 01 26.25	+04 42 19.9	+6.2;+15.7	+15.39	8.0	4.8	15	8	
38.653+0.088		19 01 35.244	+05 07 47.36	−31.8;−31.2	−31.50	1.5	0.5	19	14	
38.916−0.353		19 03 38.659	+05 09 42.49	+31.0;+33.4	+31.93	2.5	1.7	8	14	
39.100+0.491		19 00 58.04	+05 42 45.1	+12.7;+29.0	+15.80	18.6	28.3	15	6	
39.388−0.141		19 03 45.312	+05 40 42.68	+58.2;+61.5	+60.23	0.6	0.5	19	14	
40.282−0.219		19 05 41.215	+06 26 12.69	+64.8;+84.6	+73.93	16.1	41.1	8	14	
40.425+0.700		19 02 39.62	+06 59 10.5	+4.6;+16.3	+15.54	16.7	24.3	1	6	
40.623−0.138		19 06 01.63	+06 46 36.5	+29.6;+36.5	+31.10	12.9	6.3	7	6	
40.934−0.041		19 06 15.378	+07 05 54.49	+35.6;+41.6	+36.67	3.0	1.8	19	14	
41.075−0.125		19 06 49.047	+07 11 06.57	+57.0;+58.2	+57.53	0.7	0.4	19	14	
41.121−0.107		19 06 50.248	+07 14 01.49	+35.3;+37.1	+36.60	0.8	0.5	19	14	
41.123−0.220		19 07 14.856	+07 11 00.69	+55.0;+64.2	+63.39	2.2	1.9	8	14	
41.226−0.197		19 07 21.378	+07 17 08.17	+54.2;+63.0	+55.37	5.7	10.1	8	14	
41.347−0.136		19 07 21.842	+07 25 17.27	+6.8;+13.4	+11.77	14.1	19.2	17	14	
42.034+0.190		19 07 28.185	+08 10 53.47	+7.0;+15.1	+12.84	22.1	28.3	19	14	
42.303−0.299		19 09 43.592	+08 11 41.41	+26.3;+30.1	+28.08	5.2	4.3	2, 19	14	
42.435−0.260		19 09 49.858	+08 19 45.40	+66.0;+68.5	+66.69	1.9	1.6	19	14	
42.698−0.147		19 09 55.069	+08 36 53.45	−47.1;−39.0	−42.86	3.4	3.8	19	14	
43.038−0.453		19 11 38.984	+08 46 30.71	+54.1;+63.2	+54.77	5.3	6.6	8	14	
43.074−0.077		19 10 22.050	+08 58 51.49	+9.6;+11.2	+10.17	8.7	3.8	2, 19	14	
43.149+0.013	W49N	19 10 11.05	+09 05 20.4	−1.6;+23.3	+13.24	17.1	71.6	7	3	44
43.796−0.127		19 11 53.97	+09 35 53.5	+39.2;+43.5	+39.60	31.6	29.1	7	4	
43.890−0.784		19 14 26.39	+09 22 36.5	+42.8;+58.3	+47.64	8.7	17.3	1	3	
44.310+0.041		19 12 15.816	+10 07 53.52	+54.1;+57.0	+56.01	0.6	0.7	19	14	
44.644−0.516		19 14 53.766	+10 10 07.69	+48.5;+50.2	+49.50	0.9	0.5	19	14	
45.071+0.132		19 13 22.129	+10 50 53.11	+57.1;+59.8	+57.73	44.8	19.8	7	14	
45.445+0.069		19 14 18.31	+11 08 59.4	+49.3;+50.6	+49.97	1.2	0.6	4	4	45
45.467+0.053		19 14 24.15	+11 09 43.0	+55.4;+59.7	+57.45	4.5	7.9	19	4	46
45.493+0.126		19 14 11.35	+11 13 06.2	+55.7;+63.1	+57.19	7.0	6.1	4	4	47
45.804−0.356		19 16 31.081	+11 16 12.01	+59.5;+70.7	+59.92	18.1	11.1	2, 19	14	
46.066+0.220		19 14 56.077	+11 46 12.98	+22.7;+24.3	+23.53	1.0	0.7	19	14	
46.115+0.387		19 14 25.520	+11 53 25.99	+58.0;+62.6	+58.25	1.3	1.4	19	14	
48.902−0.273		19 22 10.330	+14 02 43.51	+71.3;+72.6	+71.80	0.5	0.3	19	14	48
48.990−0.299		19 22 26.134	+14 06 39.78	+70.8;+72.5	+71.48	0.7	0.5	19	14	49
49.04−1.08		19 25 22.3	+13 47 20.1	+34.7;+41.3	+36.66	25.6	37.5	13	5	
49.265+0.311		19 20 44.859	+14 38 26.91	−5.9;+7.5	−4.67	7.0	12.9	2, 19	14	
49.349+0.413		19 20 32.449	+14 45 45.44	+66.2;+69.2	+67.90	7.8	7.2	2, 19	14	
49.416+0.326		19 20 59.21	+14 46 49.6	−27.0;−9.8	−12.09	8.0	19.6	8	3	50
49.490−0.388	W51	19 23 43.95	+14 30 34.2	+47.5;+76.0	+59.27	656.9	554.6	4	4	51
49.599−0.249		19 23 26.611	+14 40 16.99	+57.3;+67.0	+63.00	41.8	86.7	8	14	
49.64−0.50		19 24 25.6	+14 35 33.9	+57.5;+60.1	+59.21	2.5	1.8	6	5	
50.03+0.58		19 21 15.1	+15 26 49.5	−10.6;−2.6	−5.19	3.1	5.2	8	13	
50.32+0.67		19 21 27.9	+15 44 20.4	+25.3;+32.0	+29.94	3.1	3.9	8	5	
50.779+0.152		19 24 17.411	+15 54 01.60	+48.0;+52.2	+49.08	4.0	3.2	19	14	
51.68+0.72		19 23 58.8	+16 57 41.0	+5.4;+8.8	+7.21	1.2	1.0	14	13	

Table A1: continued.

Name	Other name	RA(2000)	Dec(2000)	ΔV	$V_{\rm p}$	$S_{\rm p}$	$S_{\rm i}$	References		Notes
52.20+0.72		19 25 01.4	+17 25 17.4	+1.5;+4.7	+3.25	4.2	2.9	20	13	
52.663−1.092		19 32 36.07	+16 57 38.4	+64.2;+66.8	+65.83	4.7	5.0	21	3	
52.922+0.414		19 27 34.960	+17 54 38.14	+38.7;+44.9	+39.08	3.4	3.7	2, 19	14	
53.036+0.113		19 28 55.494	+17 52 03.11	+9.5;+10.5	+10.05	1.6	0.7	8	14	
53.142+0.071		19 29 17.581	+17 56 23.21	+23.4;+25.4	+24.61	2.6	1.2	8	14	
53.618+0.036		19 30 23.016	+18 20 26.68	+18.1;+19.7	+18.93	7.9	3.9	8	14	
58.77+0.64		19 38 49.1	+23 08 40.2	+30.4;+36.9	+33.22	5.7	7.4	8	13	
59.63−0.19		19 43 50.0	+23 28 36.5	+29.1;+30.5	+29.53	3.3	1.5	20	13	
59.78+0.06		19 43 11.2	+23 44 04.5	+14.2;+27.7	+26.98	34.7	51.4	7	5	
59.83+0.67		19 40 59.1	+24 04 45.8	+35.7;+39.8	+38.13	18.2	15.0	1	5	
60.57−0.19		19 45 52.3	+24 17 42.6	+2.5;+4.3	+3.64	7.4	2.5	8	5	
69.540−0.976	ON1	20 10 09.074	+31 31 35.95	−0.9;+15.8	+14.61	79.0	36.4	7	15	
70.15+1.72		20 00 54.1	+33 29 24.3	−27.1;−24.4	−26.48	5.4	5.0	6	5	
71.52−0.38		20 12 57.9	+33 30 26.5	+9.7;+11.2	+10.20	4.7	3.6	8	5	
73.06+1.80		20 08 10.2	+35 59 23.7	−4.2;+6.9	+5.91	1.6	1.8	6	5	
75.78+0.34		20 21 44.2	+37 26 36.7	−11.4;+1.6	−2.71	50.0	44.2	7	5	
78.122+3.633		20 14 26.044	+41 13 33.39	−9.4;−4.0	−7.75	34.1	51.1	12	16	
78.89+0.71		20 29 24.9	+40 11 19.2	−7.7;−6.8	−7.00	2.3	0.9	16	5	
79.736+0.991		20 30 50.67	+41 02 27.6	−6.6;−2.9	−5.47	26.7	20.6	21	3	
80.861+0.383	DR20	20 37 00.96	+41 34 55.7	−4.8;−3.4	−4.06	5.0	2.3	6	3	54
81.722+0.571	DR21(OH)	20 39 01.052	+42 22 49.18	−4.2;−2.3	−2.71	5.4	4.0	7	17	52
81.76+0.59	W75S	20 39 02.5	+42 24 59.0	−9.8;−5.2	−8.62	8.4	7.1	7	18	53
81.87+0.78	W75N	20 38 36.43	+42 37 34.8	+2.1;+10.2	+7.17	257.3	284.5	7	3	
85.41+0.00		20 54 13.7	+44 54 06.8	−33.6;−27.9	−28.53	105.3	65.4	17	5	
90.92+1.49		21 09 12.6	+50 01 02.9	−72.2;−68.2	−70.42	19.2	15.4	8	5	
94.602−1.796		21 39 58.26	+50 14 20.96	−44.3;−40.3	−40.84	5.9	6.8	6	3	
97.52+3.17		21 32 13.0	+55 52 56.0	−78.8;−67.4	−71.16	0.9	1.6	16	11	
98.04+1.45		21 43 01.5	+54 56 18.5	−62.1;−61.1	−61.58	2.1	1.0	8	5	
107.29+5.64	LDN1204A	22 21 22.5	+63 51 13.0	−11.2;−7.2	−8.53	1.4	0.9	20	11	
108.184+5.519	L1206	22 28 51.407	+64 13 41.31	−13.3;−9.6	−11.00	42.1	22.6	6	15	
108.76−0.99		22 58 47.5	+58 45 01.4	−57.2;−44.3	−45.58	3.4	3.1	8	11	
109.871+2.114	Cep A	22 56 17.903	+62 01 49.65	−5.3;−1.4	−3.75	439.4	482.6	7	19	
111.26−0.77		23 16 10.0	+59 55 31.3	−41.6;−36.2	−38.89	8.2	8.8	8	11	
111.542+0.777	NGC7538	23 13 45.364	+61 28 10.55	−62.2;−47.3	−56.03	149.3	362.7	7	20	
121.298+0.659	L1287	00 36 47.353	+63 29 02.16	−27.2;−22.0	−23.31	12.6	6.8	6	15	
123.066−6.309	NGC281	00 52 24.196	+56 33 43.17	−36.4;−27.7	−29.36	38.1	22.4	6	15	
133.947+1.064	W3(OH)	02 27 03.820	+61 52 25.40	−48.4;−41.4	−44.57	3275.	7244.	7	21	
136.84+1.15		02 49 29.8	+60 47 29.5	−45.6;−44.7	−45.24	9.7	3.7	6	5	
173.482+2.446	S231	05 39 13.059	+35 45 51.29	−15.6;−6.1	−12.98	38.1	34.5	7	10	
173.70+2.89		05 41 37.4	+35 48 49.0	−24.6;−23.4	−23.80	0.9	0.6	21	11	
174.201−0.071	AFGL5142	05 30 48.015	+33 47 54.61	−0.7;+5.1	+1.48	91.0	48.7	22	22	
183.35−0.58		05 51 11.1	+25 46 16.5	−15.6;−4.3	−4.89	13.4	8.6	6	5	
188.79+1.03		06 09 06.9	+21 50 41.7	−5.9;−4.3	−5.54	9.6	4.5	8	5	
188.946+0.886	S252	06 08 53.344	+21 38 29.16	+7.3;+12.2	+10.78	499.6	355.3	7	15	
189.030+0.784	AFGL6366	06 08 40.67	+21 31 06.9	+8.3;+11.5	+8.85	10.7	8.9	4	3	
189.77+0.34	S252A	06 08 32.4	+20 39 25.3	+3.2;+6.0	+5.42	4.5	2.7	7	5	
192.600−0.048	S255	06 12 54.020	+17 59 23.32	+1.2;+6.1	+4.57	62.3	53.1	7	15	
196.454−1.677	S269	06 14 37.051	+13 49 36.16	+14.2;+16.2	+15.14	15.6	11.6	7	15	
206.543−16.355	NGC2024	05 41 44.15	−01 54 44.9	+11.7;+12.7	+12.13	1.6	0.7	23	23	
213.705−12.597	Mon R2	06 07 47.862	−06 22 56.52	+9.6;+14.2	+10.74	350.4	184.9	7	15	
232.62+1.00		07 32 09.9	−16 58 13.1	+21.0;+23.8	+22.82	154.1	73.0	12	5	

Reference to first detection:
(**1**) Schutte et al.1993;
(**2**) unpublished data from the Torun 32m dish;
(**3**) Green et al.2010;
(**4**) Caswell et al.1995;
(**5**) Xu et al.2009;
(**6**) Slysh, Val'tts & Kalenskii 1999;
(**7**) Menten 1991;
(**8**) Szymczak et al.2000;
(**9**) Ellingsen 2007;
(**10**) Walsh et al. 1997;
(**11**) Caswell 2009;
(**12**) Macleod & Gaylard 1992;
(**13**) van der Walt et al.1995;
(**14**) Sridharan et al.2002;
(**15**) Szymczak et al.2002;
(**16**) Xu et al.2008;
(**17**) Pestalozzi et al.2005;
(**18**) Green et al.2009;
(**19**) Pandian et al. 2007;
(**20**) Fujisawa et al. 2008, private communication;
(**21**) van der Walt et al. 1996;
(**22**) Gaylard & MacLeod 1993;
(**23**) Minier et al. 2003
Reference to position:
(**1**) Walsh et al.1998;
(**2**) Green et al.2010;
(**3**) Xu et al.2009;
(**4**) Caswell 2009;
(**5**) MSX;
(**6**) Cyganowski et al.2009;
(**7**) Bartkiewicz et al.2009;
(**8**) Fuller 2007, private communication, (unpublished MERLIN data);
(**9**) Moscadelli et al. 2007;
(**10**) Green et al.2009;
(**11**) IRAS;
(**12**) Szymczak et al.2002;
(**13**) GLIMPSE;
(**14**) Pandian et al.2011;
(**15**) Rygl et al. 2010;
(**16**) Minier, Conway & Booth 2001;
(**17**) Harvey-Smith et al. 2008;
(**18**) Menten 1991;
(**19**) Sugiyama et al. 2008;
(**20**) Minier, Booth & Conway 2000;
(**21**) Etoka, Cohen & Gray 2005;
(**22**) Goddi et al. 2007;
(**23**) Minier et al. 2003
Notes:
(**1**) Confusion with the source 8.669−0.356 emission in the velocity range from +36.0 to +39.8 km s^{-1} (Green et al. 2010);
(**2**) In the velocity range from +5 to +7 km s^{-1} confusion with a weak emission of the source 9.619+0.193 (Caswell 2009);
(**3**) The emission near 10.7 km s^{-1} is a sidelobe response to the source 10.323−0.160 (Green et al.2010);
(**4**) Confusion with the sources 10.287−0.125, 10.299−0.146 and 10.342−0.142 (Walsh et al. 1998, Cyganowski et al. 2009, Green et al. 2010);
(**5**) Confusion with the sources 10.472+0.027 and 10.480+0.033 (Walsh et al. 1998, Caswell 2009, Green et al. 2010);
(**6**) Confusion with the sources 10.444−0.018 and 10.480+0.033 (Walsh et al.1998, Caswell 2009, Green et al.2010);
(**7**) Confusion with the source 10.629−0.333 (Walsh et al.1998, Green et al.2010);
(**8**) Confusion with the source 10.627−0.384 (Walsh et al.1998, Green et al.2010);
(**9**) Confusion with the sources 11.903−0.102 and 11.936−0.150 (Caswell 2009);
(**10**) Confusion with a weak emission of the source 11.919−0.613 from +37.1 to +39.5 km s^{-1} (Cyganowski et al.2009);
(**11**) Confusion with the sources 12.209−0.102 and 12.265−0.051 (Caswell 2009;

(**12**) Confusion with the sources 12.202−0.120, 12.203−0.107 and 12.181−0.123 (Caswell 2009);
(**13**) Confusion with the sources 12.209−0.102 and 12.199−0.034 (Caswell 2009);
(**14**) The emission at velocity larger than 50 km s^{-1} is a sidelobe response to the source 12.681−0.182;
(**15**) The emission centered near 40 km s^{-1} is a sidelobe response to the source 12.909−0.260;
(**16**) Confusion with the source 18.661+0.034 (Green et al.2010);
(**17**) Confusion with the sources 19.472+0.170sw and 19.486+0.151 (Caswell 2009);
(**18**) Confusion with a weak emission of the source 19.612−0.120 (Walsh et al.1998, Green et al.2010);
(**19**) Emission ranged from +60.0 to +71.0 km s^{-1} comes from the source 20.239+0.065 (Caswell 2009);
(**20**) Emission ranged from +25 to +30 km s^{-1} may come from another source;
(**21**) Emission ranged from +94 to +100 km s^{-1} comes from the source 23.440−0.182 (Caswell 2009);
(**22**) In the velocity range from 66.0 to 68.6 km s^{-1} confusion with the source 23.996−0.100 (Cyganowski et al.2009);
(**23**) Confusion with the source 24.790+0.083;
(**24**) The emission in the range 45.9 − 47.7 km s^{-1} was only reported in Cyganowski et al.2009;
(**25**) Confusion with the source 28.192+0.019 that peaks at +101.0 km s^{-1} (Walsh et. al.1998) and the source 28.201−0.049 (Caswell 2009);
(**26**) The position uncertain because of crowded region of GLIMPSE counterparts in the beam;
(**27**) Confusion with the source 29.978−0.047 that peaks at +98.2 km s^{-1} and perhaps other sources (Walsh et al.1998);
(**28**) Confusion with the source 29.955−0.016 and perhaps other sources (Walsh et al.1998);
(**29**) Confusion with the source 30.225−0.180 (Xu et al.2009);
(**30**) Confusion with the source 30.199−0.169 (Xu et al.2009);
(**31**) The emission in the range from 47.7 to 51.2 km s^{-1} probably not associated (Bartkiewicz et al.2009);
(**32**) Confusion with the source 30.757−0.048 (Walsh et al.1998);
(**33**) Confusion with the sources 30.701−0.064 and 30.816−0.052 (Walsh et al.1998);
(**34**) Confusion with the sources 30.781+0.231 and 30.791+0.205 (Walsh et al.1998);
(**35**) Confusion with the source 30.757−0.048 (Walsh et al.1998);
(**36**) Confusion with the sources 30.790+0.205 and 30.791+0.205 (Walsh et al.1998);
(**37**) Strong confusion with the source 32.04+0.06;
(**38**) The position uncertain, the emission near 60.3 km s^{-1} is probably sidelobe effect from 33.641−0.228;
(**39**) Confusion with the source 34.257+0.153 (Fuller 2007, private communication, unpublished MERLIN data), see also Caswell et al.1995);
(**40**) Confusion with the source 35.18−0.74 (Ellingsen 2007);
(**41**) The emission at velocity higher than 79.5 km s^{-1} comes from the source 37.043−0.035 (Pandian et al.2011);
(**42**) Confusion with the source 37.479−0.105 (Pandian et al. 2011);
(**43**) The emission peaked at 69.6 km s^{-1} comes from the source 37.767−0.214 (Pandian et al.2011);
(**44**) The integrated flux is given for the entire spectrum but the peak flux for the source 43.149+0.013. Confusion with the sources 43.168+0.010 (V_p=+9.3 km s^{-1}, S_p=28.4 Jy), 43.172+0.002 (V_p=+18.9 km s^{-1}, S_p=18.4 Jy), 43.170−0.007 (V_p=−1.2 km s^{-1}, S_p=2.3 Jy) and 43.178−0.014 (V_p=+11.1 km s^{-1}, S_p=0.7 Jy)(Pandian et al.2007, see also Caswell 2009 for positions of the sources);
(**45**) Confusion with the source 45.467+0.053 (Caswell 2009);
(**46**) Confusion with the source 45.445+0.069 (Caswell 2009);
(**47**) Confusion with the source 45.473+0.134 (Caswell 2009);
(**48**) Confusion with the source 48.990−0.299 (Pandian et al. 2011);
(**49**) Confusion with the source 48.902−0.273 (Pandian et al. 2011);
(**50**) Possible confusion with the source 49.417+0.324 (Cyganowski et al. 2009);
(**51**) Cluster of at least five sources: 49.470−0.371, 49.471−0.369, 49.482−0.402, 49.489−0.369 and 49.490−0.388 (Caswell 2009). Pandian et al. (2011) reported that 10 sources can be attributed to the W51 molecular cloud complex;
(**52**) The emission ranged from −4.2 to −2.3 km s^{-1} comes from DR21(OH) and is blended with the emission from the sources 81.744+0.591 (DR21(OH)N) (Harvey-Smith 2008) and 81.76+0.59 (W75S);
(**53**) Confusion with the cluster 81.722+0.571, see also Xu et al. 2009;
(**54**) The observations made for the position offset that resulted in underestimates of the flux density by more than 50%

B Spectra

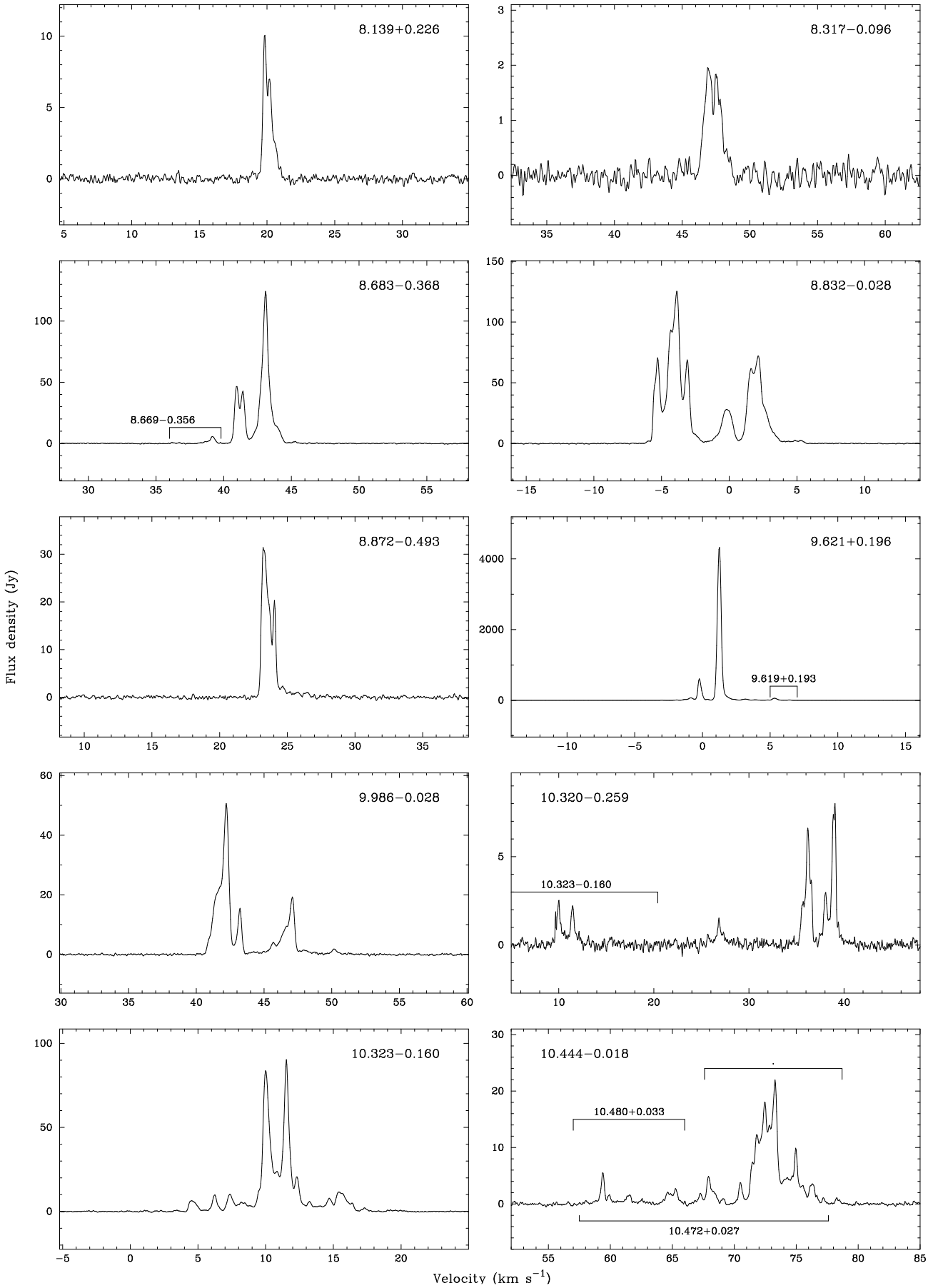

Fig. B1 Spectra of all the sources. The spectral extents are marked in many cases when blending of adjacent sources occurs.